Process Biochemistry xxx (2014) xxx–xxx

Contents lists available at ScienceDirect

Process Biochemistry

journal homepage: www.elsevier.com/locate/procbio

The inhibitory role of Co^{2+} on α-glucosidase: Inhibition kinetics and molecular dynamics simulation integration study

Xuan Li[a], Zhi-Rong Lü[b], Dong Shen[b,c], Yi Zhan[b,c], Jun-Mo Yang[d], Yong-Doo Park[b], Hai-Meng Zhou[b,c], Qing Sheng[a,*], Jinhyuk Lee[e,f,**]

[a] College of Life Sciences, Zhejiang Sci-Tech University, Hangzhou 310018, PR China
[b] Zhejiang Provincial Key Laboratory of Applied Enzymology, Yangtze Delta Region Institute of Tsinghua University, 705 Yatai Road, Jiaxing 314006, PR China
[c] School of Life Science, Tsinghua University, Zhongguancun Street, Beijing 100084, PR China
[d] Department of Dermatology, Sungkyunkwan University School of Medicine, Samsung Medical Center, Seoul 135-710, Republic of Korea
[e] Korean Bioinformation Center (KOBIC), Korea Research Institute of Bioscience and Biotechnology, Daejeon 305-806, Republic of Korea
[f] Department of Bioinformatics, University of Sciences and Technology, Daejeon 305-350, Republic of Korea

ARTICLE INFO

Article history:
Received 24 May 2014
Received in revised form 30 July 2014
Accepted 4 August 2014
Available online xxx

Keywords:
α-Glucosidase
Co^{2+}
Inhibition kinetics
Unfolding
Molecular dynamics

ABSTRACT

It is important to study enzyme inhibition of α-glucosidase (EC 3.2.1.20) due to its clinical relevance as a target enzyme for the treatment of type 2 diabetes mellitus. In this study, we investigated Co^{2+}-induced inhibition as well as structural changes of α-glucosidase integrated with computational simulations. α-Glucosidase activity was inhibited by Co^{2+} in a dose-dependent manner. Co^{2+} inhibited α-glucosidase in a parabolic non-competitive inhibition reaction ($K_i = 0.78 \pm 0.08$ mM) and directly induced regional unfolding of the enzyme resulting in a slight decrease in hydrophobic surface. The computational simulations using molecular dynamics showed that simulation with Co^{2+} resulted in a loss of secondary structure by positioning Co^{2+} near the active site for glucose production, implying that the Co^{2+} stimulate enzyme unfolding. Our study revealed the mechanism of Co^{2+} ligand binding mediated structural changes as well as inhibition of α-glucosidase activity, and suggested that Co^{2+} could act as a potent inhibitor of α-glucosidase for the treatment of type 2 diabetes mellitus.

1. Introduction

α-Glucosidase (EC 3.2.1.20) is known to hydrolyze α-(1–4)-linked D-glucose residues to α-glucoside, which is the last catalytic reaction to release glucose monomers in the digestion of carbohydrates. In this way, plasma glucose levels are directly affected by α-glucosidase activity; therefore, it is important to study inhibition of α-glucoside as the potential means of down regulating plasma glucose in patients with type 2 diabetes mellitus [1–3].

Several α-glucosidase inhibitors have been reported, such as xanthones from natural sources (*Swertia mussotii* [4]; *Tectona grandis* flowers [5]), synthetic benzohydrazide derivatives [6], and *Lactobacillus* strains present in the human gut that can reduce blood glucose responses [7,8]. These inhibitors are potential treatments for diabetes by preventing the digestion of carbohydrates and production of sugars as a result of inhibiting α-glucosidase activity. In addition to its role in the digestive process as above described, α-glucosidase also takes part in immune response in such contexts as Pompe disease [9,10], viral infection [11,12], glycoprotein trafficking [13,14], tumorigenesis [15], and several types of cancers [16–18].

Cobalt (Co^{2+}) is a transition group metal that is present in trace amounts in the human diet; however, in larger doses or chronic exposures it can be acutely toxic or cause adverse health effects [19]. It has been revealed that Co^{2+} exposure is known to directly induce gene expression and protein production including by regulating pathways related to hypoxia response and oxidative stress [20]. As an inorganic complex, Co^{2+} is regarded as useful for the development of potent and promising pharmaceutical agents due to a diverse array of manipulated properties to yield various drug candidates [21] and the best known being the role that Co^{2+} plays as a vitamin B12 cofactor [22,23].

Abbreviations: pNPG, p-nitrophenyl α-D-glucopyranoside; pNP, 4-nitrophenol; MES, 2-[N-morpholino]ethanesulfonic acid; ANS, 1-anilino-8-naphthalenesulfonate; MD, molecular dynamics.

* Corresponding author at: College of Life Sciences, Zhejiang Sci-Tech University, Hangzhou 310018, PR China. Tel.: +86 571 86843302; fax: +86 571 86843303.
** Corresponding author.
E-mail addresses: shengqing2014@hotmail.com (Q. Sheng), jinhyuk@kribb.re.kr (J. Lee).

http://dx.doi.org/10.1016/j.procbio.2014.08.002
1359-5113/

Recent studies have focused on inhibitors functions during the folding of α-glucosidase using Zn^{2+} and Ca^{2+} [24,25], and several denaturants such as urea, guanidine hydrochloride, and trifluoroethanol have also focused on conformational and activity changes [26–28]. The previous studies revealed characteristics of the α-glucosidase active site and the presence of several unfolded states and transient intermediate structures, reflecting that α-glucosidase has a stable tertiary structure. However, the relationship between α-glucosidase and Co^{2+} has not been reported, and a direct ligand binding mechanism between α-glucosidase and Co^{2+} has not been found. In this study, Co^{2+}, as an inhibitor of α-glucosidase, was applied to alter the inhibition kinetics. In addition, a molecular dynamics simulation revealed the ligand binding mechanism between Co^{2+} and α-glucosidase in detail. Results of the Co^{2+}-induced inhibitory effect, including structural changes of α-glucosidase, provide new insights into inhibition of this important enzyme and suggest possible clinical applications of Co^{2+}.

2. Materials and methods

2.1. Materials

α-Glucosidase (*Saccharomyces cerevisiae*), 4-nitrophenyl-β-D-glucuronic acid (pNPG), cobalt dichloride, 8-anilino-1-naphthalenesulfonic acid (ANS), and 2-(*N*-morpholino) ethanesulfonic acid (MES) buffer were obtained from Sigma–Aldrich (USA).

2.2. Enzyme assay

α-Glucosidase was incubated with varying concentrations of Co^{2+} (0–5.0 mM) in 50 mM MES buffer (pH 6.5) at 25 °C. The activity (v) was determined at 37 °C by measuring the change in absorbance at 400 nm using a U-3900 spectrophotometer (Hitachi, Japan), which accompanies the hydrolysis of pNPG to generate pNP according to a previously described method [27,28]. The substrate reaction mixture contained 2.5 mM pNPG substrate and 8.0 μl of enzyme solution in 1.0 ml 50 mM phosphate buffer (pH 7.2), with or without Co^{2+} at various concentrations. One unit of enzyme activity was defined as the amount of enzyme that liberated 1.0 μM of D-glucose from pNPG per minute at 37 °C (pH 7.2).

2.3. Tertiary structure measurements via intrinsic and ANS-binding fluorescence monitoring

Samples were treated for 1 h at 25 °C in incubation solutions containing different concentrations of Co^{2+}. Intrinsic fluorescence spectra were measured using an excitation wavelength of 280 nm and emission wavelengths ranging from 300 to 400 nm that were recorded using an F-2500 fluorescence spectrophotometer (Hitachi, Japan), using a 1.0 cm path length cuvette. Monitoring hydrophobic surface via ANS-binding fluorescence was performed by labeling the enzyme samples with 63 μM ANS for 40 min prior to measurement. An excitation wavelength of 380 nm was used for ANS-binding fluorescence, and emission wavelengths ranged from 400 to 600 nm. After the enzyme sample was incubated with Co^{2+} for 1 h, ANS was added to each sample. The final enzyme concentration was 2.0 μM. All reactions and measurements were carried out in 50 mM MES buffer (pH 6.5) at 25 °C.

2.4. Computational simulations

Since the structure of α-glucosidase from yeast (NCBI accession: NP_011808.1) has not been characterized by any experimentation, homology modeling was conducted using a Pseudo-Quadratic Restraint Simulated Annealing (PQR-SA) protocol [29]. The same methods were used to generate the homology model, so the developed structure was similar to one from previous work [28]. Using a generated homology model, we searched for plausible active sites using the Dockable Pocket Site Prediction (DPSP) software. Five nanosecond (ns) molecular dynamics (MD) simulations were performed in simulation conditions with and without Co^{2+}. We counted twenty Co^{2+} satisfying the experimental condition of a 10 mM concentration. A periodic boundary box size of 118 Å × 118 Å × 118 Å was used to prevent ions from moving away from the protein. A Generalized Born model of simple SWitching function (GBSW) was used to consider implicit water molecules [30]. For trajectory analyses, the Root Mean Square Deviation (RMSD) from the initial structure, the Root Mean Square Fluctuation (RMSF) as a function of residue number, and the number of bound Co^{2+} were calculated for every picosecond trajectory. All computational calculations were conducted using the CHARMM program [31]. The ratio of secondary structure (alpha/beta; units shown in percentage) was measured using the DSSP program [32].

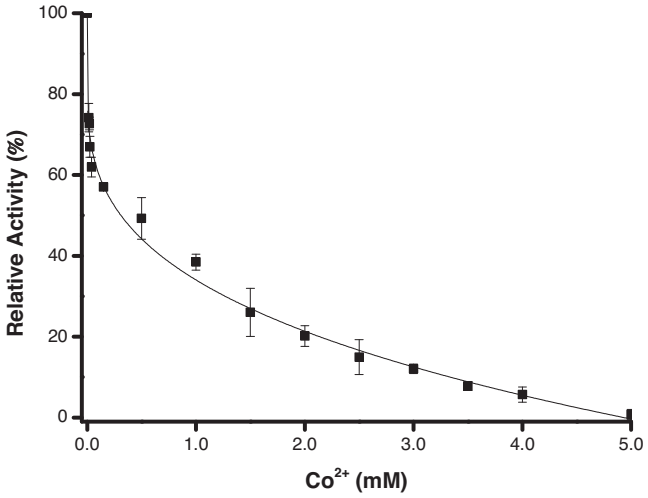

Fig. 1. Effect of Co^{2+} on the activity of α-glucosidase. The enzyme was incubated with Co^{2+} for 1 h at 25 °C. The activity was then measured by comparing with a native control enzyme and measuring the change in absorbance at 400 nm at 37 °C. The reaction mixture was composed of 2.5 mM pNPG and 8.0 μl of enzyme solution in 1.0 ml of 50 mM phosphate buffer (pH 7.2). The final enzyme concentration was 5.0 μM. Data are presented as the mean values ($n = 3$).

3. Results

3.1. Inhibitory effect of Co^{2+} on α-glucosidase activity

We found that α-glucosidase activity was inhibited in a dose-dependent manner following incubation with varying concentrations of Co^{2+} (Fig. 1). The enzyme activity was completely inactivated at a concentration of 5.0 mM Co^{2+}, and the IC_{50} (inhibitor concentration leading to a 50% loss of activity) of Co^{2+} was measured for α-glucosidase as 0.345 ± 0.01 mM ($n = 3$). This result indicates that Co^{2+} acts as a relatively strong ligand binding inhibitor for α-glucosidase.

In a subsequent experiment, we investigated the reversibility of Co^{2+}-induced inhibition by evaluating the plots of v (α-glucosidase activity) vs. various enzyme concentrations in the presence of different Co^{2+} concentrations (Fig. 2). The results revealed that all straight lines passed through the origin of point zero; these data indicate that the inhibition by Co^{2+} is reversible.

Please cite this article in press as: Li X, et al. The inhibitory role of Co^{2+} on α-glucosidase: Inhibition kinetics and molecular dynamics simulation integration study. Process Biochem (2014), http://dx.doi.org/10.1016/j.procbio.2014.08.002

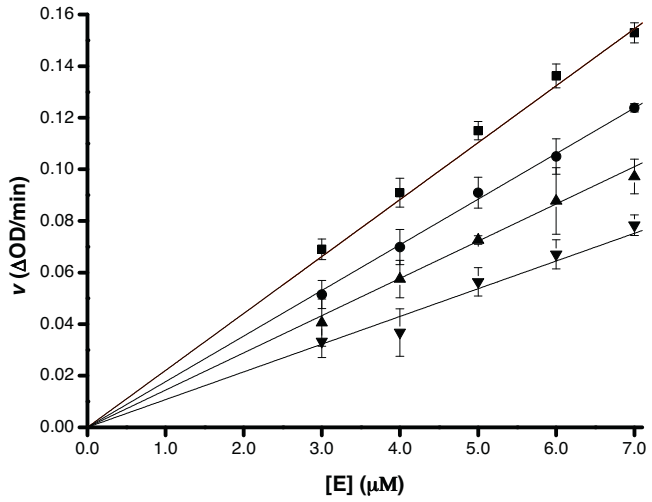

Fig. 2. The plots of v vs. [E]. The Co^{2+} concentrations were 0 (■), 0.025 (●), 0.4 (▲), and 1.0 (▼) mM, respectively. The experimental conditions were the same as for Fig. 1. [E] indicates the concentration of α-glucosidase.

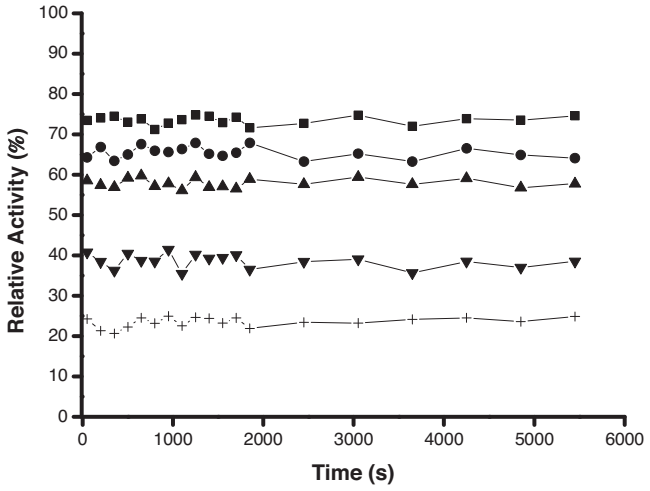

Fig. 4. Kinetic time-courses for α-glucosidase in the presence of Co^{2+}. The enzyme solution was mixed with Co^{2+} at 0.015 (■), 0.025 (●), 0.15 (▲), 1 (▼), and 2 (+) mM, respectively. The aliquots were collected at the indicated time intervals and assayed. The final enzyme and pNPG concentrations were 5.0 μM and 2.5 mM, respectively.

3.2. Study of inhibition mechanism by Co^{2+}: Lineweaver–Burk plot analysis

To evaluate the mechanism of Co^{2+}-mediated inhibition on α-glucosidase, we performed a classical kinetic Lineweaver–Burk double reciprocal analysis. We found that in the double reciprocal plots, the apparent V_{max} appeared to change significantly while the K_m value was fixed (Fig. 3), indicating that the Co^{2+}-mediated inhibition of α-glucosidase follows a non-competitive inhibition mechanism. The K_i value was calculated to be 0.78 ± 0.08 mM ($n = 3$). The double reciprocal plots demonstrated that Co^{2+} could directly bind α-glucosidase near the active site, which in turn resulted in changes to the V_{max} but not the K_m.

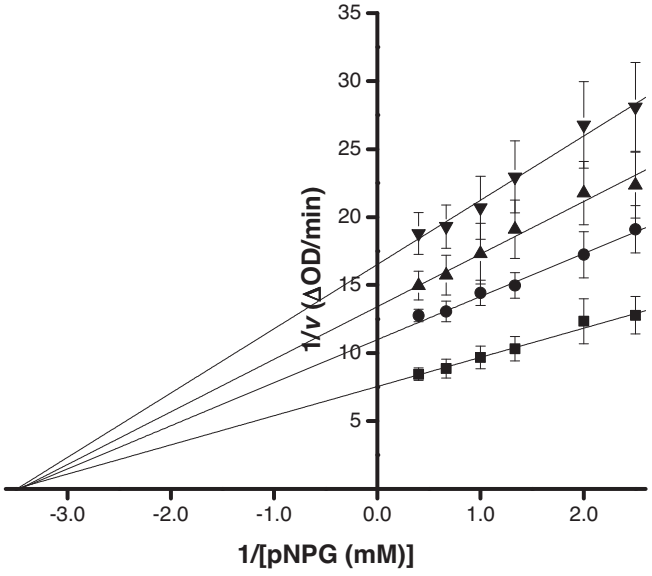

Fig. 3. Lineweaver–Burk plot. The Co^{2+} concentrations were 0 (■), 0.015 (●), 0.15 (▲), and 0.4 (▼) mM, respectively. The enzyme was incubated with Co^{2+} for 1 h at 25 °C, and then the activity was measured. The final enzyme concentration was 5.0 μM. Data are presented as the mean values ($n = 3$).

3.3. Kinetics of α-glucosidase inactivation by Co^{2+}: time-interval measurements

To determine the kinetic time-course, we performed time-interval measurements (Fig. 4). As the results indicate, there were no changes in α-glucosidase activity with timed intervals of Co^{2+} incubation from lower to higher concentrations (0.015–2.0 mM). Co^{2+} appeared to bind α-glucosidase very quickly without an apparent change of kinetic time course of inactivation. Co^{2+}-induced inactivation rapidly achieved an equilibrium state in a very short incubation time.

3.4. Conformational changes of α-glucosidase during Co^{2+}-mediated inactivation

Next, we measured the intrinsic fluorescence spectra of α-glucosidase in the presence of Co^{2+} to probe whether the α-glucosidase tertiary structural changes were induced by Co^{2+}. We observed that the fluorescence spectra intensity was significantly decreased (Fig. 5A) with maximum peak wavelength changes that were significantly red-shifted in a dose-dependent manner (Fig. 5B), showing that Co^{2+} binding to α-glucosidase directly induced tertiary structural changes. The red shift of the maximum peak approached a plateau at excessively high Co^{2+} concentrations (90 mM) where the activity was completely inactivated at this range. Compared with the results shown in Fig. 1, the concentration of Co^{2+} required to induce structural changes in α-glucosidase is greater than the concentration required to achieve a loss of enzymatic activity, indicating that the loss of activity induced by Co^{2+} is more sensitive than the loss of tertiary structure.

To monitor changes to the hydrophobic surface as a result of structural changes induced by Co^{2+}, we measured the ANS-binding fluorescence spectra (Fig. 6). Our results demonstrate that ANS-fluorescence intensity of α-glucosidase decreased slightly in a dose-dependent manner with increasing Co^{2+} concentrations. Interestingly, compared to the results demonstrating intrinsic fluorescence change, the hydrophobic surface of α-glucosidase was slightly changed and not exposed by Co^{2+} binding. Because hydrophobic surface changes are associated with conformational changes in the active site, we deduced that the shape of the active site pocket was slightly changed. However, the active site change

Please cite this article in press as: Li X, et al. The inhibitory role of Co^{2+} on α-glucosidase: Inhibition kinetics and molecular dynamics simulation integration study. Process Biochem (2014), http://dx.doi.org/10.1016/j.procbio.2014.08.002

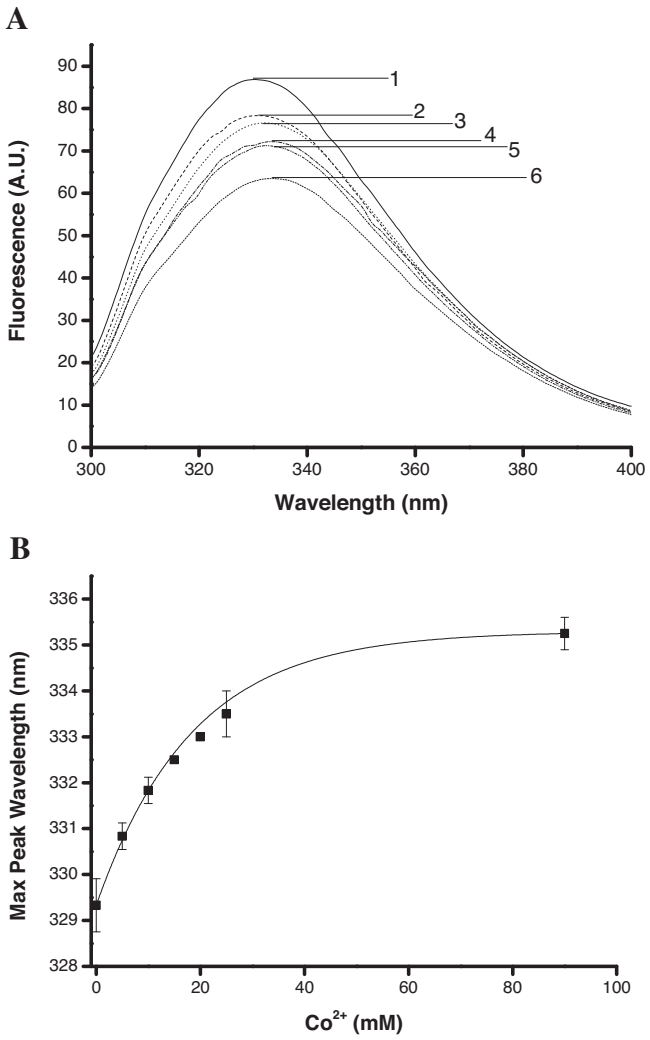

Fig. 5. Intrinsic fluorescence spectra changes of α-glucosidase induced by Co^{2+}. (A) The enzyme was incubated with different concentrations of Co^{2+} for 1 h. The final enzyme concentration was 2.0 μM. The excitation wavelength was 280 nm. The Co^{2+} concentrations for curves 1–6 were 0, 5, 10, 15, 20, and 25 mM, respectively. (B) Secondary replot of the maximum wavelength versus Co^{2+}. The experimental conditions were the same as for (A). Data are presented as the mean values ($n = 3$).

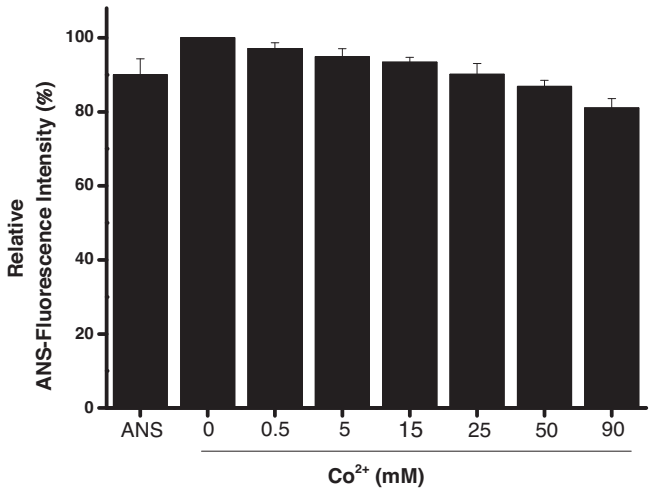

Fig. 6. ANS-binding fluorescence intensity change of α-glucosidase induced by Co^{2+}. ANS (63 μM) was incubated for 40 min to label the hydrophobic surface of α-glucosidase prior to the measurement after incubation with Co^{2+} for 1 h. The final concentration of the enzyme was 2.0 μM. The excitation wavelength was 380 nm. Label 1 indicates ANS background without incubating with the enzyme. Labels 2–8 indicate concentrations of Co^{2+} at 0, 0.5, 5, 15, 25, 50, and 90 mM, respectively.

could not directly induce substrate accessibility and docking to the catalytic reactive residues, which was monitored by the unchanged K_m value in Fig. 3. The combination of results from intrinsic and ANS-binding fluorescence experiments gave us insight into the conformational state of α-glucosidase in the presence of Co^{2+} where it did not induce whole level structural changes but rather local regional changes by decreasing surface hydrophobicity. Thus, the conformational change in the active site induced by Co^{2+} was mainly to be synchronized with the loss of catalytic function but it was less effectively to the overall structural change of the enzyme.

3.5. Molecular dynamic simulations of Co^{2+} and α-glucosidase

Two molecular dynamics simulations with and without Co^{2+} were performed during 5-ns intervals. The RMSD time profile of two simulations is shown in Fig. 7A. The RMSD in the simulation with Co^{2+} plateaued within 1 ns while the simulation without Co^{2+} plateaued in 2 ns. Because Co^{2+} can bind to the negative residues of a protein and restrict protein motion (flexibility), the number of bound Co^{2+} was measured as a function of simulation time (Fig. 7B). Five ions were already bound at the initial structure and another five ions were quickly bound at the initial step of molecular dynamics (~50 ps). Finally, twelve ions were bound to the protein after 1 ns and eight ions were free in the aqueous environment. Both RMSD time profiles (Fig. 7A) and the number of bound Co^{2+} (Fig. 7B) were similar in that the two quickly increased by 1 ns and kept their states from 1 ns to the final 5 ns. These data imply that the binding of Co^{2+} to the protein may make the protein more rigid.

The initial and final structures with Co^{2+}, generated from the MD simulations, are shown in Fig. 8. In the initial structure, Co^{2+} were randomly distributed (Fig. 8A). In the final structure (Fig. 8B), twelve ions were bound to the proteins and eight ions (in the black circles) were still unbound. The most secondary structures of the initial structure were lost in the final structure. The alpha/beta ratio was changed from 26.5/14.4 (the initial structure) to 9.4/0.7 (the final structure), implying that the Co^{2+} trigger unfolding of α-glucosidase as they penetrate into the core of the protein although the RMSD of the structure was constant during the simulation.

The secondary structure schemes from two final structures with and without Co^{2+} were compared (Fig. 9A). The two final structures lost the most secondary structures relative to the initial structure. In particular, the final structure with Co^{2+} lost secondary structure (alpha/beta = 9.4/0.7) by 4.1% relative to the structure without Co^{2+} (11.5/2.7). To qualify the flexibility of the protein motion, RMSFs of two MD simulations were measured (Fig. 9B). RMSF shows flexibility of proteins during MD simulations with (red line) and without (green line) Co^{2+} (Fig. 9B). The protein without Co^{2+} had more flexibility, in particular in N- and C-terminals, whereas the bound Co^{2+} could make the protein more rigid because the docked residues with Co^{2+} (red boxes in Fig. 9B below) were generally positioned at the low RMSF values (red line in Fig. 9B). The fact that the bound Co^{2+} contribute to less flexibility in the protein is consistent with the previous time profile result shown in Fig. 7. The DPSP method identified a plausible pocket site (Fig. 9C) that ACG called "pentasaccharide" based on the Protein Data Bank (PDB). The ACG binding residues were MET69, TYR71, PHE177, ARG212, ASP214, GLU276, HIS348, ASP349, and ARG439. These residues may comprise a plausible active site for glucose production. The residues (blue boxes) are located close to the interacting regions of the Co^{2+} in the final structure (red boxes in Fig. 9B below), indicating that the Co^{2+}

Please cite this article in press as: Li X, et al. The inhibitory role of Co^{2+} on α-glucosidase: Inhibition kinetics and molecular dynamics simulation integration study. Process Biochem (2014), http://dx.doi.org/10.1016/j.procbio.2014.08.002

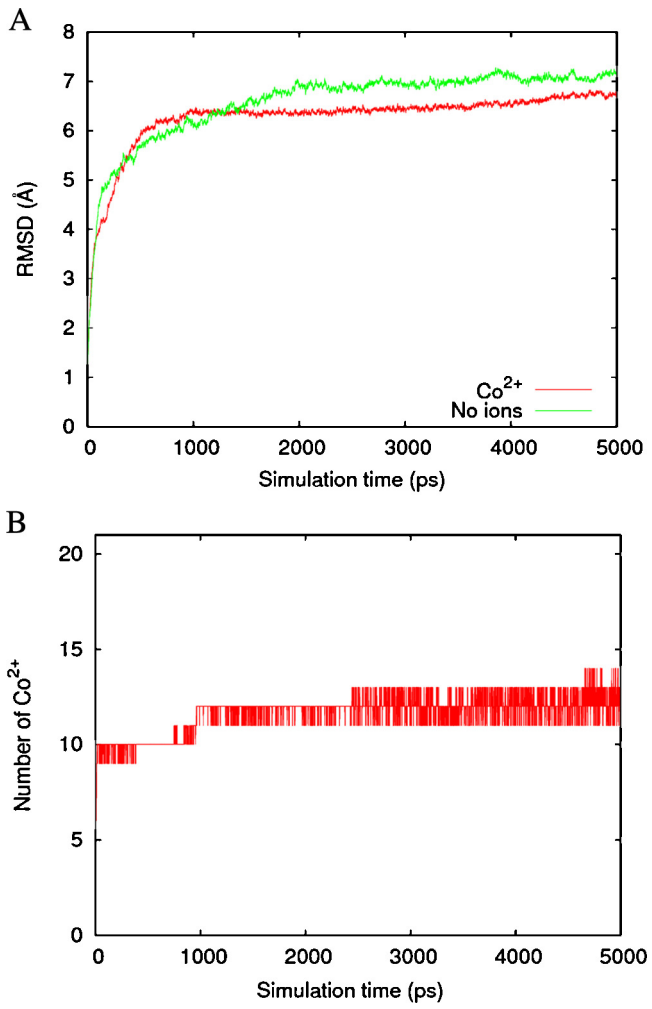

Fig. 7. Trajectory analyses of molecular dynamics simulations. (A) Root Mean Square Deviation of Carbon alpha (Cα) with the reference structure of the initial structure at 0 ns. RMSDs of simulations with (red line) and without (green line) Co^{2+} were measured every 1 ps. The *X*-axis is the simulation time from 0 to 5 ns (5000 ps) and the *Y*-axis is the RMSD (Å). (B) The number of bound Co^{2+} to α-glucosidase during the MD simulations. The *X*-axis is the simulation time from 0 to 5 ns and the *Y*-axis is the number of Co^{2+} to the protein. The number of bound Co^{2+} is counted when the Co^{2+} ion approaches within 5 Å from the protein. (For interpretation of the references to color in this figure legend, the reader is referred to the web version of this article.)

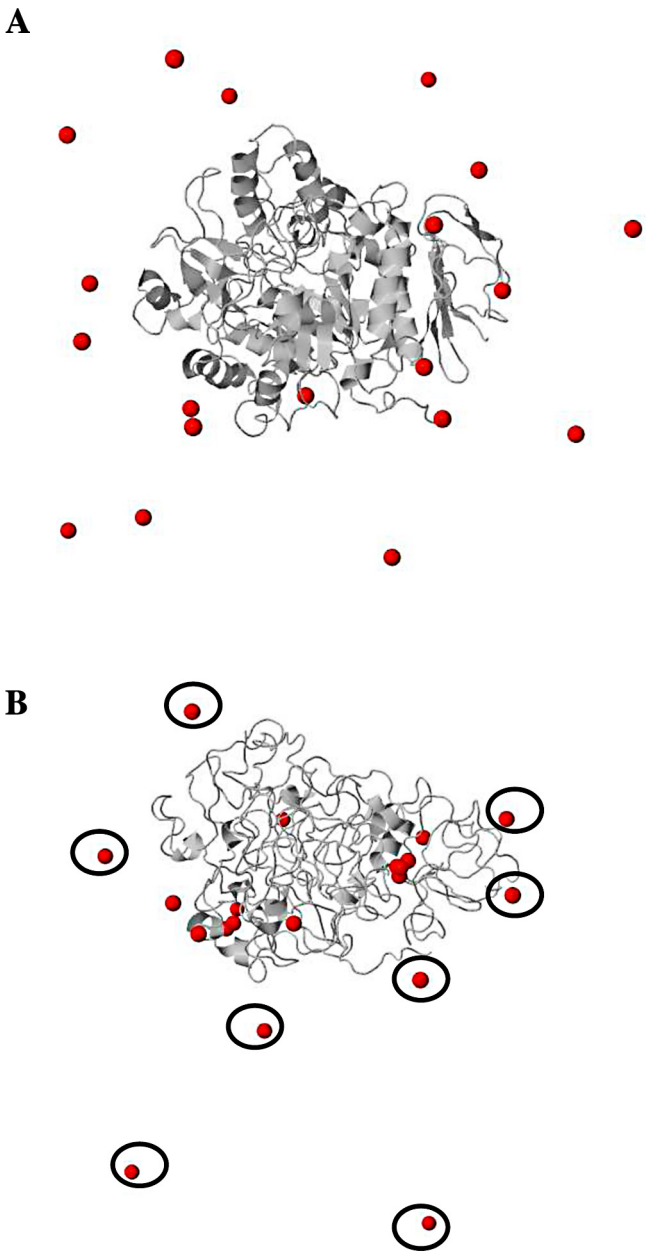

Fig. 8. MD structures. (A) Initial structure of the simulation with Co^{2+} and (B) the final α-glucosidase structure. The proteins are drawn by a gray cartoon image and the Co^{2+} are shaded using a red space-fill model. In (B), the unbound Co^{2+} to the protein are drawn by red circles. (For interpretation of the references to color in this figure legend, the reader is referred to the web version of this article.)

can pre-occupy the regulatory site and block the enzyme catalytic reaction.

4. Discussion

From our studies on inhibition kinetics, we discovered that Co^{2+} effectively inhibits α-glucosidase, following a typical non-competitive inhibition mechanism. Co^{2+} binding also induces the active site structure of α-glucosidase. It is not clear whether the Co^{2+}-mediated conformational change is the more energetically favored state; however, the catalytic activity of α-glucosidase in this state clearly showed complete loss after Co^{2+} binding. In comparison to the reaction concentration of Co^{2+}, a higher concentration of Co^{2+} is needed to regulate the tertiary structure of α-glucosidase, and this observation indicates that the active site responds to Co^{2+} in a manner that is distinct from the overall structure.

Co^{2+}-induced inhibition is non-competitive in that partial α-glucosidase unfolding likely affects the enzyme-substrate state in the Co^{2+} bound state, as displayed by a change in V_{max}, but simultaneously does not affect the substrate binding in the active site, as reflected by no change in K_m value. This might be due to the flexible active site response to Co^{2+} binding on the docking site of α-glucosidase.

Computational simulations show that the Co^{2+} play a role in unfolding α-glucosidase. These simulations are supported by trajectory analyses from the MD simulations (e.g. RMSD, RMSF, and the number of bound Co^{2+} plot). The results are also used to support experimental kinetic studies.

In conclusion, we revealed the effect of Co^{2+} on α-glucosidase inhibition as well as the mechanism of Co^{2+} binding to α-glucosidase at the molecular level by integrating computational simulations. Co^{2+} may be useful as a potent dietary supplement for treating type 2 diabetes mellitus.

Please cite this article in press as: Li X, et al. The inhibitory role of Co^{2+} on α-glucosidase: Inhibition kinetics and molecular dynamics simulation integration study. Process Biochem (2014), http://dx.doi.org/10.1016/j.procbio.2014.08.002

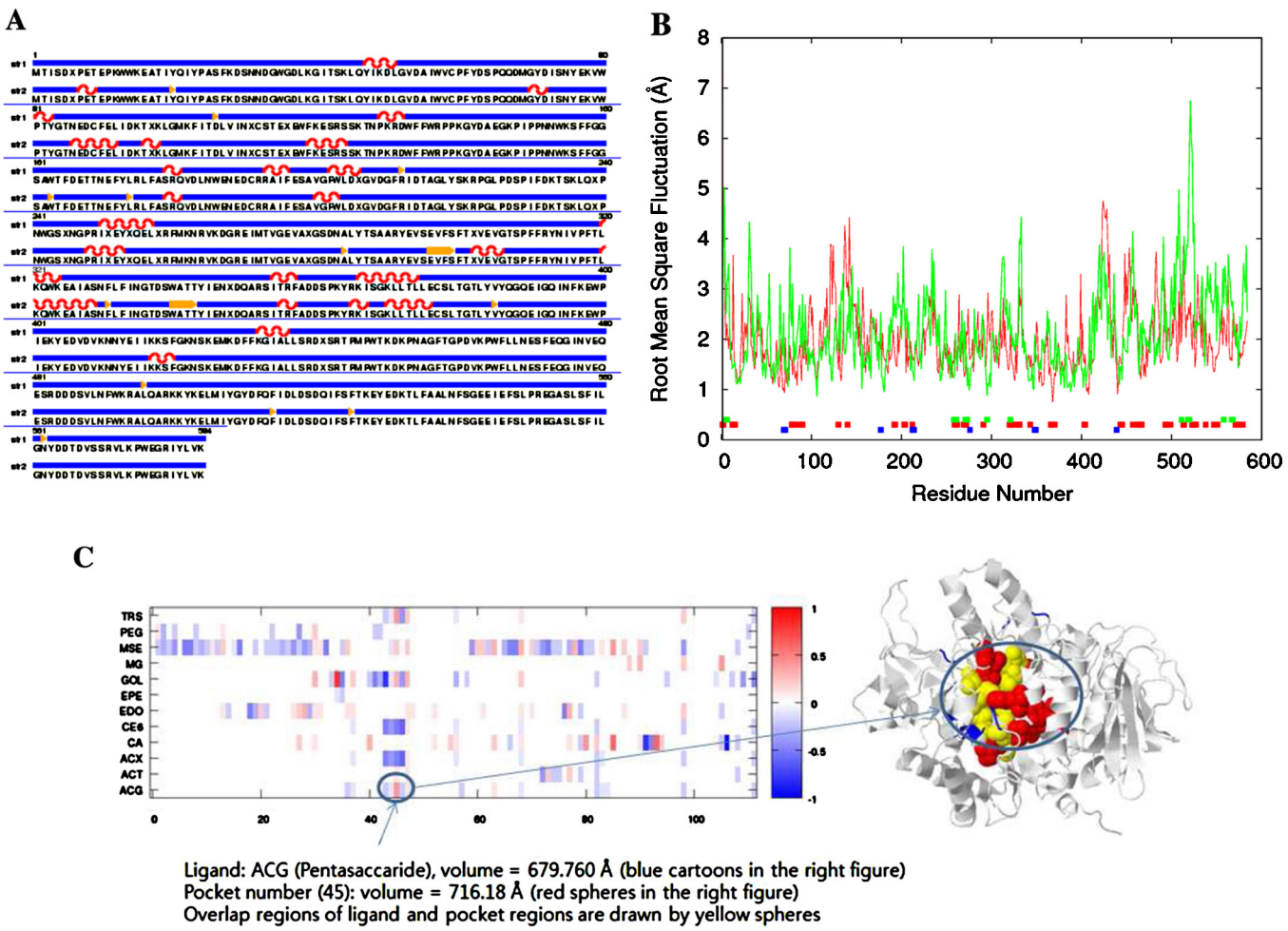

Fig. 9. Protein secondary structure and RMSF plots. (A) The secondary structure schemes of the two final structures from 5 ns MD simulations with (structure 1) and without (structure 2) Co^{2+}. The helix, beta, and coil structures are drawn by red, yellow, and blue cartoon images, respectively. (B) The RMSF plot from two simulations with (red line) and without (green line) Co^{2+}. The predicted ACG binding residues are marked by blue boxes below. The docked residues of Co^{2+} from the final and initial structures are marked by red and green boxes, respectively. (C) The circle in the right structure figure is a plausible binding position. The circle has higher correlation score (red) between pocket number 45 and ACG ligand (pentasaccharide). (For interpretation of the references to color in this figure legend, the reader is referred to the web version of this article.)

Acknowledgments

This study was supported by the China Natural Science Foundation No. 31170732 and No. 31270854. Dr. Hai-Meng Zhou was supported by the fund from Science and Technology of Xiaoshan District No. 2012121 and by the fund from the Science and Technology Bureau of Jiaxing No. 2012AY1040. Dr. Zhi-Rong Lü was supported by a grant from the Science and Technology Planning Project of Hangzhou (No. 20120232B39). Dr. Jun-Mo Yang was supported by a grant from the Korea Health Technology R&D Project, Ministry of Health & Welfare, Republic of Korea (No. HI12C1299) and by a grant from the Samsung Biomedical Research Institute (GL1-B2-181-1). Dr. Yong-Doo Park was supported by a grant from Zhejiang Provincial Natural Science Foundation of China, "Toward studying the function of C3dg protein and elucidating its role in the pathogenesis of atopic dermatitis" (Grant No. LY14H110001). Dr. Jinhyuk Lee was supported by grants from the Korea Research Institute of Bioscience and Biotechnology (KRIBB) Research Initiative Program, the Korean Ministry of Education, Science and Technology (MEST) (2012R1A1A2002676), and the Pioneer Research Center Program through the National Research Foundation of Korea funded by the Ministry of Science, ICT & Future Planning (2013M3C1A3064780).

References

[1] Scheen AJ. Is there a role for alpha-glucosidase inhibitors in the prevention of type 2 diabetes mellitus. Drugs 2003;63:933–51.
[2] Servey JT. Alpha-glucosidase inhibitors may reduce the risk of type 2 diabetes. Am Fam Physician 2007;76:374–5.
[3] van de Laar FA. Alpha-glucosidase inhibitors in the early treatment of type 2 diabetes. Vasc Health Risk Manag 2008;4:1189–95.
[4] Luo CT, Zheng HH, Mao SS, Yang MX, Luo C, Chen H. Xanthones from *Swertia mussotii* and their α-glycosidase inhibitory activities. Planta Med 2014;80:201–8.
[5] Ramachandran S, Rajasekaran A. Blood glucose-lowering effect of Tectona grandis flowers in type 2 diabetic rats: a study on identification of active constituents and mechanisms for antidiabetic action. J Diabetes 2014.
[6] Khan MS, Munawar MA, Ashraf M, Alam U, Ata A, Asiri AM, et al. Synthesis of novel indenoquinoxaline derivatives as potent α-glucosidase inhibitors. Bioorg Med Chem 2014;22:1195–200.
[7] Panwar H, Calderwood D, Grant IR, Grover S, Green BD. Lactobacillus strains isolated from infant faeces possess potent inhibitory activity against intestinal alpha- and beta-glucosidases suggesting anti-diabetic potential. Eur J Nutr 2014.
[8] Panwar H, Rashmi HM, Batish VK, Grover S. Probiotics as potential biotherapeutics in the management of type 2 diabetes – prospects and perspectives. Diabetes Metab Res Rev 2013;29:103–12.
[9] Wang Z, Okamoto P, Keutzer J. A new assay for fast, reliable CRIM status determination in infantile-onset Pompe disease. Mol Genet Metab 2014;111:92–100.
[10] Cousens LP, Mingozzi F, van der Marel S, Su Y, Garman R, Ferreira V, et al. Teaching tolerance: new approaches to enzyme replacement therapy for Pompe disease. Hum Vaccin Immunother 2012;8:1459–64.

Please cite this article in press as: Li X, et al. The inhibitory role of Co^{2+} on α-glucosidase: Inhibition kinetics and molecular dynamics simulation integration study. Process Biochem (2014), http://dx.doi.org/10.1016/j.procbio.2014.08.002

[11] Chapel C, Garcia C, Roingeard P, Zitzmann N, Dubuisson J, Dwek RA, et al. Antiviral effect of alpha-glucosidase inhibitors on viral morphogenesis and binding properties of hepatitis C virus-like particles. J Gen Virol 2006;87:861–71.
[12] Chapel C, Garcia C, Bartosch B, Roingeard P, Zitzmann N, Cosset FL, et al. Reduction of the infectivity of hepatitis C virus pseudoparticles by incorporation of misfolded glycoproteins induced by glucosidase inhibitors. J Gen Virol 2007;88:1133–43.
[13] Alonzi DS, Kukushkin NV, Allman SA, Hakki Z, Williams SJ, Pierce L, et al. Glycoprotein misfolding in the endoplasmic reticulum: identification of released oligosaccharides reveals a second ER-associated degradation pathway for Golgi-retrieved proteins. Cell Mol Life Sci 2013;70:2799–814.
[14] Alonzi DS, Neville DC, Lachmann RH, Dwek RA, Butters TD. Glucosylated free oligosaccharides are biomarkers of endoplasmic-reticulum alpha-glucosidase inhibition. Biochem J 2008;409:571–80.
[15] Zwerschke W, Mannhardt B, Massimi P, Nauenburg S, Pim D, Nickel W, et al. Allosteric activation of acid alpha-glucosidase by the human papillomavirus E7 protein. J Biol Chem 2000;275:9534–41.
[16] Lai SW, Liao KF, Lai HC, Tsai PY, Sung FC, Chen PC. Kidney cancer and diabetes mellitus: a population-based case–control study in Taiwan. Ann Acad Med Singapore 2013;42:120–4.
[17] Chen YL, Cheng KC, Lai SW, Tsai IJ, Lin CC, Sung FC, et al. Diabetes and risk of subsequent gastric cancer: a population-based cohort study in Taiwan. Gastric Cancer 2013;16:389–96.
[18] Lai SW, Liao KF, Chen PC, Tsai PY, Hsieh DP, Chen CC. Antidiabetes drugs correlate with decreased risk of lung cancer: a population-based observation in Taiwan. Clin Lung Cancer 2012;13:143–8.
[19] Paustenbach DJ, Tvermoes BE, Unice KM, Finley BL, Kerger BD. A review of the health hazards posed by cobalt. Crit Rev Toxicol 2013;43:316–62.
[20] Permenter MG, Dennis WE, Sutto TE, Jackson DA, Lewis JA, Stallings JD. Exposure to cobalt causes transcriptomic and proteomic changes in two rat liver derived cell lines. PLOS ONE 2013;8:e83751.
[21] Heffern MC, Yamamoto N, Holbrook RJ, Eckermann AL, Meade TJ. Cobalt derivatives as promising therapeutic agents. Curr Opin Chem Biol 2013;17:189–96.
[22] Tiffany ME, Fellner V, Spears JW. Influence of cobalt concentration on vitamin B12 production and fermentation of mixed ruminal microorganisms grown in continuous culture flow-through fermentors. J Anim Sci 2006;84:635–40.
[23] Heldt D, Lawrence AD, Lindenmeyer M, Deery E, Heathcote P, Rigby SE, et al. Aerobic synthesis of vitamin B12: ring contraction and cobalt chelation. Biochem Soc Trans 2005;33:815–9.
[24] Zeng YF, Lee J, Si YX, Yan L, Kim TR, Qian GY, et al. Inhibitory effect of Zn^{2+} on α-glucosidase: inhibition kinetics and molecular dynamics simulation. Process Biochem 2012;47:2510–7.
[25] Zhang X, Shi L, Li X, Sheng Q, Yao L, Shen D, et al. Effect of Ca^{2+} on the activity and structure of α-glucosidase: inhibition kinetics and molecular dynamics simulations. J Biosci Bioeng 2014;117:696–705.
[26] Wu XQ, Xu H, Yue H, Liu KQ, Wang XY. Inhibition kinetics and the aggregation of alpha-glucosidase by different denaturants. Protein J 2009;28:448–56.
[27] Wu XQ, Wang J, Lü ZR, Tang HM, Park D, Oh SH, et al. Alpha-glucosidase folding during urea denaturation: enzyme kinetics and computational prediction. Appl Biochem Biotechnol 2010;160:1341–55.
[28] Zeng YF, Lü ZR, Yan L, Oh S, Yang JM, Lee J, et al. Towards alpha-glucosidase folding induced by trifluoroethanol: kinetics and computational prediction. Process Biochem 2012;47:2284–90.
[29] Kim TR, Oh S, Yang JS, Lee S, Shin S, Lee J. A simplified homology-model builder toward highly protein-like structures: an inspection of restraining potentials. J Comput Chem 2012;33:1927–35.
[30] Im W, Lee MS, Brooks 3rd CL. Generalized born model with a simple smoothing function. J Comput Chem 2003;24:1691–702.
[31] Brooks BR, Brooks 3rd CL, Mackerell Jr AD, Nilsson L, Petrella RJ, Roux B, et al. CHARMM: the biomolecular simulation program. J Comput Chem 2009;30:1545–614.
[32] Kabsch W, Sander C. Dictionary of protein secondary structure: pattern recognition of hydrogen-bonded and geometrical features. Biopolymers 1983;22:2577–637.

Please cite this article in press as: Li X, et al. The inhibitory role of Co^{2+} on α-glucosidase: Inhibition kinetics and molecular dynamics simulation integration study. Process Biochem (2014), http://dx.doi.org/10.1016/j.procbio.2014.08.002